FATIGUE DELAMINATION INITIATION IN L-BEND CFRP COUPONS

J. P. Blanchfield*[1], G. Allegri[1]

[1]*Advanced Composites Centre for Innovation and Science (ACCIS), Aerospace Engineering, University of Bristol, University Walk, BS8 1TR, Bristol, UK*
* *Corresponding Author: jamie.blanchfield@bristol.ac.uk*

Keywords: Composites, SN-curves, Curved beams, Initiation,

Abstract
Accurate modelling of the delamination of composites due to cyclic loading is important to reduce the costs associated with fatigue testing of structures. This work aims to identify the point of damage initiation in a carbon-fibre laminate subject to pure interlaminar tensile cyclic loading for a range of severities and stress ratios, in order to generate full SN-curves for an aerospace-grade carbon-fibre epoxy composite. Curved beams have been used in 4-point bend tests roughly in line with the ASTM D 6415 test standard to generate the required failure conditions. The tests were monitored in-situ using an Acoustic Emissions system and post-test CT (X-Ray) Scans were employed to identify failure conditions in the specimens.

1. Introduction

The low through-thickness strength of composites means that delamination failure at the interface between plies is a common failure mode for composite structures. Cyclic loading of these structures can lead to damage onset and growth. The fatigue life of composites can be usefully split into two phases: an initiation phase during which time microscopic cracks are coalescing to the point at which an observable crack is formed, and then a propagation phase, during which time the crack grows to a maximum acceptable length.

The majority of progressive fatigue damage models focus on the propagation phase, assuming that a crack is already present in the material. They therefore neglect the time spent before the initiation of damage, which in many cases can be significant [1]. Hence these models tend to provide a conservative estimate of the overall fatigue life. In order to improve prediction accuracy, there have been attempts to develop models that can account for both the initiation and the propagation phases. One approach is to treat propagation as a series of stepwise-initiations, thereby unifying the two phases into one coherent analysis [2].

A recently developed fatigue damage evolution model based upon this approach has been able to provide the material SN-curves for initiation of damage under pure mode II fatigue loading in a moderately tough carbon fibre reinforced composite (CFRP), and has shown that fatigue delamination propagation can be predicted from this initiation data alone [3]. In order to extend this model to mixed-mode conditions, it has been necessary to obtain data for the initiation of

fatigue damage due to pure interlaminar tension. One of the main methods for ascertaining the through thickness tensile strengths of laminated composites is to use curved beams under bending to produce the through-thickness stresses [4]. In this research an ASTM standard static test method using L-shaped curved beams has been employed under cyclic loading [5].

Issues arising from the use of this test method in both static and fatigue testing are discussed and results are presented. Because the damage evolution law mentioned above attempts to predict fatigue delamination growth rates from initiation data, it is important to identify the point of fatigue 'initiation' as accurately as possible in a given material. Since, by definition, to identify damage initiation one must first have a pristine material, obtaining experimental data for initiation stresses in a material is not a trivial matter, even for quasi-static testing, because of the sensitivity to manufacturing defects in the test region. Seon et al [6] approach this problem by characterising voids in individual specimens. In this work, the approach has been to manufacture good quality specimens to minimise the occurrence of stress concentrations around voids. Additionally, specimens in which the failure could not be fairly attributed to interlaminar tension in the test region were discounted. Although this led to a high proportion of discounted specimens, it led to a simple post-processing of results.

2. Experimental Programme

2.1. Specimen Preparation

The specimens were manufactured by hand layup of IM7/8552 prepreg over a male tool as described in [7]. The specimens were cut to widths of 11mm and were 32 plies thick, with an average laminate thickness of 4.05mm. The material elastic properties as used in the stress calculations were $E_{11} = 161GPa, E_{22} = 11.38GPa$, and $\nu_{12} = 0.32$, where the subscripts 11 and 22 represent the circumferential and radial directions, respectively, in the curved region of the specimen, and axial and through thickness directions, respectively, in the specimen legs. Several batches of panels were produced, including material from two different rolls of prepreg.

2.2. Test Setup

In order to produce interlaminar tensile stresses, the specimen is subjected to 4-point bending on smooth rollers (Figure 1). The experimental setup is as prescribed in [5], which also cites the method of calculating the maximum interlaminar stress at failure. In [7] a correction was applied to this stress calculation in order to account for specimen deformation during the test, and it was demonstrated that without this correction, the error in the calculation of maximum stress would be approximately 10%. The same correction has also been applied in this work.

The test method is designed so that, under quasi-static loading, failure is sudden and catastrophic rather than gradual so that the precise point of delamination initiation can be easily identified. In order to ensure this is also the case in the fatigue tests, *in-situ* monitoring of the specimen was initially carried out using a Vallen Acoustic Emissions system. In this work it was found that, although it was not possible using this system to completely rule out damage initiation in the specimen prior to final failure under cyclic loading, the information from the acoustic emissions in conjunction with the compliance data from the test machine strongly indicated that generally failure occurred suddenly rather than gradually(see Section 2.4).

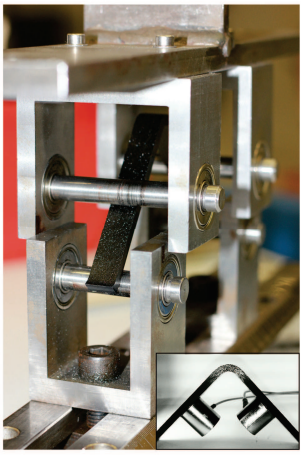

Figure 1. Rig used for the static and fatigue testing. *Inset:* the acoustic emissions sensors attached to the specimen.

Roll	Strength [MPa]	CV [%]
A	109.1	17.8
B	110.3	11.8
A+B	109.7	14.2

Table 1. Interlaminar strengths obtained from curved beam specimens using material from two different rolls.

2.3. Static Test Results

A summary of the results from the static tests is given in Table 1. The mean static strength from the static tests as described in [7] was found to be 109.7 MPa. This is higher than the manufacturer's quoted transverse tensile strength of 64MPa [8], but no value for *interlaminar* tensile strength is given. The overall coefficient of variation (CV) was 14.2%, but was significantly higher for specimens from manufactured from Roll A than those from Roll B. Five specimens from each roll were tested, and although the mean static strength was very similar for both sets of specimens, the CV for Roll A specimens was higher than that for Roll B. A possible cause for this is that at least two of the specimens from Roll A were cut from the end of panels, where manufacturing defects are more likely to occur and the location on the panel of the other three specimens is unknown.

2.3.1. Error analysis

There are two possible sources of the large CV in these tests: experimental error from single tests, such as measurement errors, and variation in actual specimen strength due to defects within the curved region, such as stress concentrations around voids. In order to quantify the effect of experimental error, an error analysis as suggested in [9], can be carried out. The sources of experimental error for a single test can be seen in Figure 2. Although there are large uncertainties in the elastic properties of the material, these have a negligible effect on the overall calculation of stress. Conversely, despite a relatively small uncertainty in the values of l_b, l_t(the distance between the top and bottom rollers respectively), and t_c(the specimen thickness

in the curved region), these can have a large effect on the predicted failure stress. The overall uncertainty in a single test due to experimental error, is calculated to be 8.2%, which means that this accounts for the majority of CV of 11.8% in the static test results of specimens tested from Roll B.

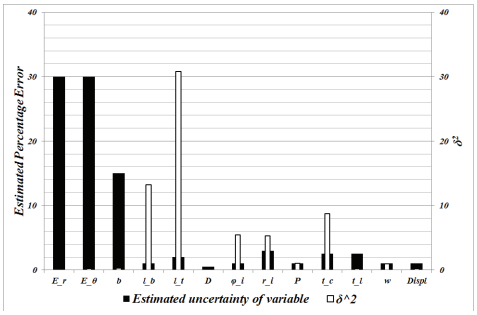

Figure 2. Sources of experimental errors in a single test. The black columns correspond to estimated error in each variable, and the white columns show that error's effect on the overall calculation of radial stress (δ^2). ϕ_i is the initial angle between the specimen legs, r_i is the inner radius of the curved region, t_l is the thickness of the specimen legs, b is a the distance between upper and lower rollers parallel to the specimen leg, and *Displ* is the crosshead displacement.

2.3.2. CT(X-Ray) Inspection of Specimens

The analysis of Section 2.3.1 suggests that the manufacturing quality in the curved region of specimens away from the edge of the panels is good and is unlikely to be the sole or even the major cause of the strength variation in the tests. In order to investigate the state of the curved laminate, CT(X-Ray) inspection of this region was carried out. The scans were carried out on specimens that had been subjected to cyclic loading. Because it was desired to continue cyclic testing after the scans, no dye-penetrant was used on the specimens as this can affect the interfacial properties. To see whether damage or defects would be visible without dye-penetrant, a specimen with a known matrix split and delamination was inspected. The results can be seen in the upper image of Figure 3 that clearly shows the expected damage. In contrast, no significant voids, wrinkling, delaminations or matrix splitting was discovered in any of the five specimens inspected, a typical example of which can be seen in the lower image of Figure 3. Because these scans are all from specimens that had endured fatigue testing without failure, they may be artificially skewing the results toward specimens that do not have defects, therefore further CT-scans are needed on untested specimens to be more certain of the defect-free state of the test region. However, the evidence so far, from the error analysis and from the CT-scans, indicates an acceptable level of manufacturing quality to be able to calculate failure stresses without the need for taking into account effects of stress concentrations around individual defects.

2.4. Fatigue Testing

2.4.1. Test setup

Fatigue tests were carried out at two stress ratios and at a range of severities. The severity was calculated by dividing the average peak stress throughout the test by the mean static strength, and the stress ratio was defined as the average minimum stress throughout the test divided by

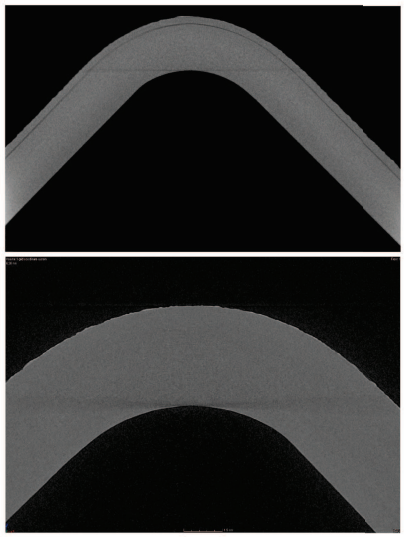

Figure 3. CT(X-Ray) scans of curved beams, without the use of dye-penetrant. Matrix splits can be clearly distinguished (above). In contrast, no significant voids or ply-wrinkling were observed in any of the five specimens inspected after fatigue tests, an example of which is shown in the lower image.

the average peak stress. The frequency of the tests was varied between 4.1-7.9 Hz to keep the stressing rate constant for each test.

The tests were initially run in load control, however, early on in the programme it became apparent that some specimens were failing by matrix splitting on the upper surface prior to delamination and final failure. As a result, fatigue testing was switched to displacement control because, under load control, the loss of stiffness due to the matrix split would lead to an increase in crosshead displacement for a given load, and subsequent rapid failure. This rapid failure, instigated from a matrix split would be difficult to distinguish from a genuine instantaneous delamination. In contrast, under displacement control, the matrix split would cause a loss of stiffness which could be detected prior to final failure.

2.4.2. Detection of Damage

Any delamination originating from a matrix split cannot be considered a valid failure, so detection of these matrix splits was crucial. This was performed by monitoring peak loads; deviations from a plateau were an indication of damage in the specimen, and matrix splitting could subsequently usually be confirmed visually after stopping the test. In addition, an Acoustic Emissions (AE) system was used to attempt to detect damage events, such as delamination initiation *in-situ*. However, for these tests, it was deemed insufficiently accurate to detect and locate any potential individual delamination initiation events, and so was used only in conjunction with the peak load data to aid detection of matrix splitting.

Because the AE system was not used for detecting potential delamination events, post-test

CT(X-Ray) scans of five specimens were taken. The specimens had all undergone fatigue testing, enduring between 52′000 and 1.0^6 cycles. No evidence of damage was found in any of the specimens (see Figure 3).

2.4.3. Fatigue Test Results

The ultimate aim of this work was to generate SN-curves for the initiation of delamination in IM7/8552 due to pure interlaminar tension, at more than one stress ratio. From the evidence shown in Section 2.4.2 it can be assumed that no delamination initiation event occurs during the fatigue tests prior to final failure, and therefore it is this final failure that is taken as the point of damage initiation on the SN curves that follow. The stress at which the final failure occurs is calculated from the mean of the peak loads and displacements during the fatigue test, which should both (excepting noise) remain constant throughout. This assumes that failure occurs in the area of maximum stress in the curved region of the specimen. Figure 4 shows the radial stress distribution through the thickness of the laminate in the curved region. The maximum stress occurs at approximately 40% through the thickness from the lower surface of the specimen. However, the stress remains within one standard deviation of the mean static strength within the range 25-60% of the through thickness, which will be referred to as the *maximum stress region*. Failure usually leads to multiple delaminations, making identification of the initiation site difficult, however there are usually one or two main delaminations which extend further into the specimen legs than smaller delaminations. Previous authors [10] have taken these to be the *initial* delaminations. Following this principle, it can be also be seen in Figure 4 that of the 23 specimens that suffered final failure, 17 of the failures occurred within the maximum stress region. Of the six failures that initiated outside the maximum stress region, all of them occurred above this region, and none higher than 80% of the thickness. A discussion of whether to accept these six results as valid follows later in this section.

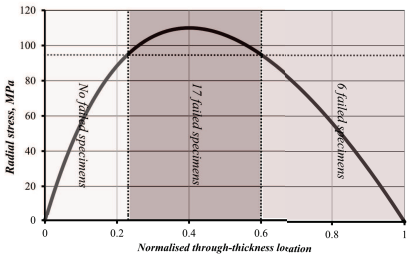

Figure 4. Interlaminar tensile stress distribution through the specimen thickness for a given maximum stress of 110MPa. The maximum stress occurs at approximately 40% through the thickness from the lower surface of the specimen. The stress remains within one standard deviation mean static strength within the range 25-60% of the through thickness. Also shown is how many specimens failed inside or outside this range.

The SN curves produced from the fatigue testing of the curved beam specimens is shown in Figure 5. There was considerable scatter in the results, which was expected given the variation in the mean static strength, which is shown as the grey band on the figure. The experimental data has been fitted with a non-linear curve fit to an analytical model described in Section 3 over the entire data set using MATLAB®'s *nlinfit* tool. The curve fit shows that generally fatigue endurance of the specimens increases with decreasing severity. This effect is more marked for

a stress ratio of R=0.1 (larger amplitude) than for R=0.5, which is to be expected for this more punishing fatigue regime.

As mentioned above, six of the specimens were deemed to have delaminated at locations between 60-80% of the laminate thickness, and therefore at a theoretical stress less than one standard deviation from the predicted stress. Of these six specimens, three failed at a number of cycles greater than the average, that is, *above* the material SN curve, implying that the material at the maximum stress location (40%) endured a even greater than average number of cycles than expected. It was therefore decided not to discount these six results because this might artificially skew the SN curves, making them unconservatively shallow.

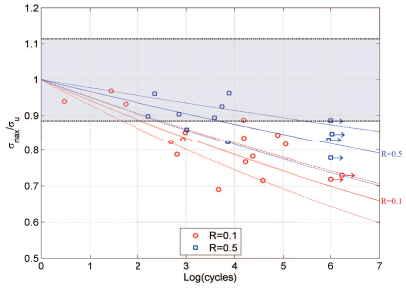

Figure 5. SN-curves produced from the fatigue testing of the curved beam specimens. The grey band represents 1 s.d. from the mean of the static failure strength, and the dashed lines represent 1 s.d. from the mean of the model fit

3. Application of Experimental Results

In [3] a non-linear fatigue damage model was proposed that was capable of providing material SN curves for interlaminar shear damage initiation for a range of stress ratios, and simultaneously the crack growth rates under similar mode II loading. It is here proposed to use the same model to fit SN curves to the experimental data generated in this work for pure interlaminar tension. By fitting the the entire experimental dataset (R=0.1 & 0.5) to Equation 1, the following model parameters were obtained: $b = 34.810 \pm 5.494, \kappa = 0.990 \pm 0.359$. These curves are significantly shallower than the equivalent mode II curves found in [3], which highlights the importance of considering the number of cycles to delamination initiation when predicting overall fatigue life of a composite structure.

$$\frac{\sigma_{max}}{\sigma_u} = N_f^{-(1-R)^{\kappa}/b} \tag{1}$$

4. Conclusions and further work

This work has been conducted in order to develop a fatigue delamination evolution model. SN data for the initiation of delamination in a carbon fibre epoxy composite under pure interlaminar tension has been generated, using curved beams under bending to generate the required stress field.

The SN curves generated were relatively shallow, highlighting the significant proportion of overall fatigue life that can be endured before delamination initiates, especially under higher stress ratios. The experimental data has been fitted to a power curve type model, and it is hoped that this data can be used to predict mode I fatigue delamination growth rates in the same material.

Acknowledgements

The authors are grateful to Rolls-Royce Plc. for having supported this research through the Composites University Technology Centre at the University of Bristol, and also to the Engineering and Physical Sciences Research Council (EPSRC) - EPSRC grant number EP/G036772/1.

References

[1] M. Quaresimin and M. Ricotta. Fatigue behaviour and damage evolution of single lap bonded joints in composite materials. *Compos Sci Technol*, 66:176–87, 2006.

[2] J. Andersons, M. Hojo, and S. Ochiai. Model of delamination propagation in brittle-matrix composites under cyclic loading. *J Reinforced Plast Compos*, 20(5):431–50, 2001.

[3] G. Allegri and M. Wisnom. A non-linear damage evolution model for mode ii fatigue delamination onset and growth. *Int J Fatigue*, 43:226–34, 2012.

[4] R. Olsson. A survey of test method for multiaxial and out-of-plane strength of composite laminates. *Compos Sci Tech*, 71:773–83, 2011.

[5] ASTM. Standard Test Method for Measuring the Curved Beam Strength of a Fiber-Reinforced Polymer-Matrix Composite. *ASTM D6415-99*, 2004.

[6] Guillaume Seon, Andrew Makeev, Yuri Nikishkov, and Edward Lee. Effects of defects on interlaminar tensile fatigue behavior of carbon/epoxy composites. *Composites Science and Technology*, 89:194–201, December 2013.

[7] J. Blanchfield and G. Allegri. Delamination initiation due to interlaminar tension in fibre-reinforced plastics. In *The 19th International on Composite Materials*, pages 7078–86. ICCM19, July 2013.

[8] Hexcel Composites. Hexply®8552 product data sheet. `http://www.hexcel.com/Resources/DataSheets/Prepreg-Data-Sheets/8552_eu.pdf`, February 2013.

[9] C. Jackson and H. Martin. An Interlaminar Tensile Strength Specimen. In *Composite Materials*, volume 11, pages 333–54. 1993.

[10] R.H. Martin. Delamination failure in a unidirectional curved composite laminate. NASA Contractor Report 182018, April 1990.